

# Dynamics Modelling and Simulation of Super Truss Element based on Non-linear Beam Element

Lingchong Gao, Xiaobing Dai, Michael Kleeberger and Johannes Fottner  
*Chair of Materials Handling, Material Flow, Logistics, Technical University of Munich, Boltzmannstrasse 15,  
85748 Garching, Germany*

**Keywords:** Non-Linear Dynamics, Mobile Crane, Lattice Boom, Model Reduction.

**Abstract:** A mobile crane equipped with a lattice boom system is widely used to lift the heavy load on construction sites. Even though the lattice structure can provide strong support with limited mass, the inertia force of the lattice boom is still not neglectable, so is the heavy lifting load. Therefore, the dynamic response of the lattice boom is important but also time-consuming due to a large number of degrees of freedom. In engineering, the truss beam is often simplified as a continuous beam, but because of the noncontinuity of the truss, this direct modelling method cannot truly reflect the actual dynamics of the truss. In this paper, a detailed Super Truss Element formulation for nonlinear truss elements is proposed to reduce the number of degrees of freedom. The formulation uses nonlinear spatial Timoshenko Beam based on co-rotational coordinate and dynamic condensation approach with three assumptions. After parameterizing the characteristics of the Super Truss Element, a nonlinear method for the calculation of the mass matrix and force vector in a large displacement and rotation is developed. A dynamic simulation of the spatial motion of the lattice boom crane is performed and the results are analysed.

## 1 INTRODUCTION

Among the large number of cranes developed for various tasks, mobile cranes are particularly flexible in their application possibilities. Truck-mounted cranes, mobile cranes, railway cranes, and crawler cranes are different cranes equipped with a boom system, their booms can be designed as telescopic or truss booms. Compared with the continuous boom structure, the crane with a truss boom has a higher load capacity under the same mass due to the optimization of its structure. It is suitable for lifting tasks with special requirements for lifting height and radius. It is mainly used for large-scale factory construction, steel, and building construction. (Kleeberger 1996)

The form of cranes is diverse and complex. In the design process, simulation and proofreading for different types of cranes under different load cases are required, which causes many calculations. As a kind of engineering machinery, mobile cranes need to lift a large load and move. Considering the mass of the hoisting cargo and the boom structure, dynamics calculations should be done, especially for some extreme conditions in the holistic capacity sheet. The

dynamic modeling of lattice boom becomes difficult due to the unevenness of cross-section and a large number of nodes and elements. Previously there are mainly two modeling methods:

1. Modeling of each element of the lattice boom. The model will be closer to the actual lattice boom, but due to a large number of nodes, the overall model has a large number of degrees of freedom (Günthner und Kleeberger 1997). This decreases the solution speed and efficiency.

2. Modeling the entire lattice boom with a continuous flexible beam element. This method can greatly reduce the number of degrees of freedom and accelerate the calculation of the system, but without the necessary theoretical basis, the accuracy of the model will be decreased.

Therefore, a scientific reduction method that accelerates the model calculation and makes the number of degrees of freedom small is urgently needed.

For truss boom, there is a static condensation method, which condenses the stiffness and gravity of the truss beam to the nodes on the end section. This method is only suitable for the static reduction of linear models (Kleeberger und Hübner 2006).

For dynamics reduction, the Craig-Bampton method is often used. It converts the dynamic equations from the time domain into the frequency domain to obtain information such as the natural frequency of the system (Koutsovasilis und Beiteltschmidt 2007). However, for nonlinear models, it is very difficult to convert them to the frequency domain (Kammer et al. 2015).

In this paper, a super truss element with only two nodes is proposed based on three assumptions. Under the premise that the total energy of the super truss element is the same as the actual truss model, this element can condense the mass matrix and force vector of each flexible body, normally each pipe, in the truss. Therefore, the number of degrees of freedom of the entire truss can be reduced to 12 and solving speed of dynamic calculation can be increased.

## 2 SUPER TRUSS ELEMENT

### 2.1 Spatial Timoshenko Beam based on Co-rotational Formulation

The large deformation of the truss element is caused by the cumulative effects of small deformation from elements in the truss. Therefore, we model each element in the truss as a short beam with small linear deformation. Here spatial Timoshenko beam based on co-rotational formulation is used to model the beam element of the truss.

#### 2.1.1 Co-rotational Coordinate

The co-rotational coordinate describes the position of the element without deformation. The deformation of any point on the element is based on the co-rotational coordinate.

The co-rotational coordinate  $\mathbf{q}_B$  can be defined by the coordinates of the two ends of the element, where the script "B" represents the co-rotational coordinate system (base coordinate system), the script "e" represents the element coordinate system and the script "I" represents the inertial coordinate system.

$$\mathbf{q}_B = \begin{bmatrix} {}_I\mathbf{r}^{B^T} & \boldsymbol{\varphi}^{B^T} \end{bmatrix}^T = \mathbf{q}_B(\mathbf{q}_e) \quad (1)$$

$$\mathbf{q}_e = [q_1^T \quad q_2^T]^T$$

where  ${}_I\mathbf{r}^B$  is the position vector of the origin point of co-rotational coordinate expressed in inertial coordinate, and  $\boldsymbol{\varphi}^B$  is the Cartesian vector for co-rotational coordinate.

The relationship between the generalized velocity  $d\mathbf{q}_B$  and acceleration  $d\dot{\mathbf{q}}_B$  of the co-rotational coordinate and the generalized velocity  $d\mathbf{q}_e$  and acceleration  $d\dot{\mathbf{q}}_e$  of the end-point coordinates can be expressed as

$$\begin{aligned} d\mathbf{q}_B &= \begin{bmatrix} {}_I\dot{\mathbf{r}}^{B^T} & {}_B\boldsymbol{\omega}^{B^T} \end{bmatrix}^T = \mathbf{T}_B d\mathbf{q}_e \\ d\dot{\mathbf{q}}_B &= \mathbf{T}_B d\dot{\mathbf{q}}_e + \dot{\mathbf{T}}_B d\mathbf{q}_e \end{aligned} \quad (2)$$

$\mathbf{q}_B$ ,  $\mathbf{T}_B$  and  $\dot{\mathbf{T}}_B$  can be determined according to the definition of co-rotational coordinate system.

#### 2.1.2 The Formulation of Deformation

According to the Timoshenko beam assumption, the deformation of any point on the section  $c$  is caused by the centroid translational deformation of the section  ${}_B\mathbf{u}^c$  and the section rotational deformation  ${}_B\boldsymbol{\psi}^c$ . The actual deformation of this point  ${}_B\mathbf{u}$  can be obtained by the difference between the position vector before deformation  ${}_I\mathbf{r}^*$  and the after deformation  ${}_I\mathbf{r}$ ,

$$\begin{aligned} {}_I\mathbf{r}^* &= {}_I\mathbf{r}^B + \mathbf{R}_B({}_B\mathbf{r}^c + {}_c\mathbf{t}) \\ {}_I\mathbf{r} &= {}_I\mathbf{r}^B + \mathbf{R}_B({}_B\mathbf{r}^c + {}_B\mathbf{u}^c + \mathbf{R}_{d,c}{}_c\mathbf{t}) \end{aligned} \quad (3)$$

where  ${}_B\mathbf{r}^c$  is the relative position of cross-section  $c$  to the original point of co-rotational coordinate, and  ${}_c\mathbf{t}^T = [0 \quad {}_cy \quad {}_cz]$  is the relative position of any point on cross-section  $c$  to the sectional centre.  ${}_B\mathbf{r}^c$  and  ${}_c\mathbf{t}$  are constant for each cross-section.

Here we use the hypothesis of small rotational deformation. The subscript "d" represents the deformation coordinate. The rotation matrix  $\mathbf{R}_{d,c}$  for axis-angle rotation vector  ${}_B\boldsymbol{\psi}^c$  can be written as:

$$\mathbf{R}_{d,c} \approx \mathbf{I} + {}_B\tilde{\boldsymbol{\psi}}^c \quad (4)$$

where  $\tilde{\mathbf{a}}$  represents the skew symmetric matrix of the corresponding vector  $\mathbf{a}$ .

Thus, the deformation can be approximated as

$${}_B\mathbf{u} = \mathbf{R}_B^T({}_I\mathbf{r} - {}_I\mathbf{r}^*) \approx {}_B\mathbf{u}^c + {}_B\tilde{\boldsymbol{\psi}}^c {}_c\mathbf{t} \quad (5)$$

The deformation coordinate of the end point  $\mathbf{q}_{d,end}$  can be expressed by the following formula

$$\begin{cases} {}_B\mathbf{u}^e = \mathbf{R}_B^T({}_I\mathbf{r}^e - {}_I\mathbf{r}^B) - {}_B\mathbf{r}^e \\ {}_B\boldsymbol{\psi}^e = {}_B\boldsymbol{\psi}^e(\mathbf{R}_B^T\mathbf{R}_e) = {}_B\boldsymbol{\psi}^e(\mathbf{R}_{d,e}) \end{cases} \quad (6)$$

$$\mathbf{q}_{d,end} = [{}_B\mathbf{u}^{1^T} \quad {}_B\boldsymbol{\psi}^{1^T} \quad {}_B\mathbf{u}^{2^T} \quad {}_B\boldsymbol{\psi}^{2^T}]^T$$

The velocity and acceleration of the deformation at the end point can be expressed by element coordinate.

$$\begin{aligned} d\mathbf{q}_{d,\text{end}} &= \mathbf{T}_{d,\text{end}} d\mathbf{q}_e \\ &= [\mathbf{B}\dot{\mathbf{u}}^1 \quad \mathbf{1}\dot{\boldsymbol{\omega}}^1 \quad \mathbf{B}\dot{\mathbf{u}}^2 \quad \mathbf{2}\dot{\boldsymbol{\omega}}^2]^T \end{aligned} \quad (7)$$

$$d\dot{\mathbf{q}}_{d,\text{end}} = \mathbf{T}_{d,\text{end}} d\dot{\mathbf{q}}_e + \dot{\mathbf{T}}_{d,\text{end}} d\mathbf{q}_e \quad (8)$$

where  $\mathbf{1}\dot{\boldsymbol{\omega}}^i$  represent the angular velocity of the angular deformation  $\mathbf{B}\boldsymbol{\psi}^i$ .  $\mathbf{T}_{d,\text{end}}$  and  $\dot{\mathbf{T}}_{d,\text{end}}$  can be obtained through equation (6).

The deformation coordinate  $\mathbf{q}_{d,c}$  is defined as

$$\mathbf{q}_{d,c} = [\mathbf{B}\mathbf{u}^c \quad \mathbf{B}\boldsymbol{\psi}^c]^T \quad (9)$$

### 2.1.3 Kinematics of Points on the Beam

The velocity and acceleration of the point on the beam after the deformation is depend on the generalized velocity and acceleration of co-rotational coordinate and deformation coordinate, which can be written as

$$\begin{aligned} \dot{\mathbf{r}} &= (\mathbf{H}_t + \mathbf{H}_{r,t}) \begin{bmatrix} d\mathbf{q}_B \\ d\mathbf{q}_{d,c} \end{bmatrix} \\ \ddot{\mathbf{r}} &= (\mathbf{H}_t + \mathbf{H}_{r,t}) \begin{bmatrix} d\dot{\mathbf{q}}_B \\ d\dot{\mathbf{q}}_{d,c} \end{bmatrix} \\ &\quad + (\mathbf{D}_t + \mathbf{D}_{r,t}) \begin{bmatrix} d\mathbf{q}_B \\ d\mathbf{q}_{d,c} \end{bmatrix} \end{aligned} \quad (10)$$

where  $\mathbf{H}_t$  and  $\mathbf{D}_t$  provide the translational velocity and acceleration of the beam cross-section. They can be formulated as

$$\begin{aligned} \mathbf{H}_t &= [\mathbf{H}_{t,B} \quad \mathbf{H}_{t,d,c}] \\ \mathbf{D}_t &= [\mathbf{D}_{t,B} \quad \mathbf{D}_{t,d,c}] \end{aligned} \quad (11)$$

in which

$$\begin{aligned} \mathbf{H}_{t,B} &= [\mathbf{I} \quad -\mathbf{R}_B(\mathbf{B}\tilde{\mathbf{r}}^c + \mathbf{B}\tilde{\mathbf{u}}^c)] \\ \mathbf{D}_{t,B} &= [\mathbf{0} \quad -\mathbf{R}_{BB}\tilde{\boldsymbol{\omega}}^B(\mathbf{B}\tilde{\mathbf{r}}^c + \mathbf{B}\tilde{\mathbf{u}}^c)] \\ \mathbf{H}_{t,d,c} &= [\mathbf{R}_B \quad \mathbf{0}] \\ \mathbf{D}_{t,d,c} &= [2\mathbf{R}_{BB}\tilde{\boldsymbol{\omega}}^B \quad \mathbf{0}] \end{aligned}$$

And  $\mathbf{H}_{r,t}$  and  $\mathbf{D}_{r,t}$  provide the rotational velocity and acceleration of the beam cross-section around the axis where  $c\mathbf{t}$  is located

$$\begin{aligned} \mathbf{H}_{r,t} &= \mathbf{H}_r(c\mathbf{t}) = [\mathbf{H}_{r,t,B} \quad \mathbf{H}_{r,t,d,c}] \\ \mathbf{D}_{r,t} &= \mathbf{D}_r(c\mathbf{t}) = [\mathbf{D}_{r,t,B} \quad \mathbf{D}_{r,t,d,c}] \end{aligned} \quad (12)$$

in which

$$\begin{aligned} \mathbf{H}_{r,t,B} &= [\mathbf{0} \quad -\mathbf{R}_{cc}\tilde{\mathbf{t}}\mathbf{R}_{d,c}^T] \\ \mathbf{H}_{r,t,d,c} &= [\mathbf{0} \quad -\mathbf{R}_{cc}\tilde{\mathbf{t}}] \\ \mathbf{D}_{r,t,B} &= [\mathbf{0} \quad -\mathbf{R}_{BB}\tilde{\boldsymbol{\omega}}^B\mathbf{R}_{d,c}\tilde{\mathbf{t}}\mathbf{R}_{d,c}^T\tilde{\mathbf{t}}] \\ \mathbf{D}_{r,t,d,c} &= [\mathbf{0} \quad -(\mathbf{2}\mathbf{R}_{BB}\tilde{\boldsymbol{\omega}}^B\mathbf{R}_{d,c} + \mathbf{R}_{cc}\tilde{\boldsymbol{\omega}}^c)\tilde{\mathbf{t}}] \end{aligned}$$

### 2.1.4 The Formulation of Strain and Stress

The strain at this point is defined using linear Green-Lagrange strains, which is defined as the derivative of the deformation with respect to the coordinate.

$$\mathbf{B}\boldsymbol{\varepsilon}_{ij} = \frac{1}{2} \left( \frac{\partial_B u_i}{\partial_c x_j} + \frac{\partial_B u_j}{\partial_c x_i} \right) \quad (13)$$

in details

$$\begin{cases} \mathbf{B}\boldsymbol{\varepsilon}_{xx} = \mathbf{B}u^{c'} - \mathbf{B}\theta^{c'}_c y + \mathbf{B}\psi^{c'}_c z \\ \mathbf{B}\boldsymbol{\varepsilon}_{xy} = \frac{1}{2} (\mathbf{B}v^{c'} - \mathbf{B}\varphi^{c'}_c z - \mathbf{B}\theta^c) \\ \mathbf{B}\boldsymbol{\varepsilon}_{xz} = \frac{1}{2} (\mathbf{B}w^{c'} + \mathbf{B}\varphi^{c'}_c y + \mathbf{B}\psi^c) \\ \mathbf{B}\boldsymbol{\varepsilon}_{yy} = \mathbf{B}\boldsymbol{\varepsilon}_{yz} = \mathbf{B}\boldsymbol{\varepsilon}_{zz} = 0 \end{cases}$$

where

$$\begin{aligned} \mathbf{B}\mathbf{u}^c &= [\mathbf{B}u^c \quad \mathbf{B}v^c \quad \mathbf{B}w^c]^T \\ \mathbf{B}\boldsymbol{\psi}^c &= [\mathbf{B}\varphi^c \quad \mathbf{B}\psi^c \quad \mathbf{B}\theta^c]^T \end{aligned}$$

and  $(\cdot)' = \partial(\cdot)/\partial_c x$ .

Through the constitutive relationship between stress and strain, we can get

$$\mathbf{B}\boldsymbol{\sigma}_{ij} = \begin{cases} E_B \boldsymbol{\varepsilon}_{ij}, i = j \\ G_B \boldsymbol{\varepsilon}_{ij}, i \neq j \end{cases} \quad (14)$$

### 2.1.5 The Virtual Power of Beam Element

The virtual internal power of the element can be expressed as

$$\begin{aligned} \delta p_{\text{int}} &= - \iiint_V \sum_i \sum_j \delta \mathbf{B}\boldsymbol{\varepsilon}_{ij} \mathbf{B}\boldsymbol{\sigma}_{ij} dV \\ &= - \int_0^L \delta \dot{\mathbf{q}}_{d,c}^T (\mathbf{H}_1 \mathbf{q}'_{d,c} + \mathbf{H}_2 \mathbf{q}_{d,c}) ds \\ &\quad + \int_0^L \delta \dot{\mathbf{q}}_{d,c}^T (\mathbf{H}_3 \mathbf{q}'_{d,c} + \mathbf{H}_4 \mathbf{q}_{d,c}) ds \end{aligned} \quad (15)$$

The integration by parts is used to deal with the first part of the integration

$$\begin{aligned} \delta p_{\text{int}} = & -\delta \dot{\mathbf{q}}_{\text{d},c}^T (\mathbf{H}_1 \mathbf{q}'_{\text{d},c} + \mathbf{H}_2 \mathbf{q}_{\text{d},c}) \Big|_0^L \\ & + \int_0^L \delta \dot{\mathbf{q}}_{\text{d},c}^T (-\mathbf{H}_1 \mathbf{q}''_{\text{d},c} + (\mathbf{H}_3 - \mathbf{H}_2) \mathbf{q}'_{\text{d},c} \\ & + \mathbf{H}_4 \mathbf{q}_{\text{d},c}) ds \end{aligned} \quad (16)$$

The virtual inertial power of the beam element can be expressed as

$$\begin{aligned} \delta p_{\text{ine}} = & - \iiint_V \delta \dot{\mathbf{r}}^T \rho \dot{\mathbf{r}} dV \\ = & - \int_0^L \delta \begin{bmatrix} d\mathbf{q}_B \\ d\mathbf{q}_{\text{d},c} \end{bmatrix}^T \left( \mathbf{M}_{\text{B},c} \begin{bmatrix} d\dot{\mathbf{q}}_B \\ d\dot{\mathbf{q}}_{\text{d},c} \end{bmatrix} \right. \\ & \left. + \mathbf{D}_{\text{B},c} \begin{bmatrix} d\mathbf{q}_B \\ d\mathbf{q}_{\text{d},c} \end{bmatrix} \right) ds \end{aligned} \quad (17)$$

The mass matrix and damping matrix regarding to co-rotational coordinate and deformation coordinate of cross-section  $c$  can be formulated as

$$\begin{aligned} \mathbf{M}_{\text{B},c} = & \rho A \mathbf{H}_t^T \mathbf{H}_t + \rho I_y \mathbf{H}_{r,y}^T \mathbf{H}_{r,y} \\ & + \rho I_z \mathbf{H}_{r,z}^T \mathbf{H}_{r,z} \\ \mathbf{D}_{\text{B},c} = & \rho A \mathbf{H}_t^T \mathbf{D}_t + \rho I_y \mathbf{H}_{r,y}^T \mathbf{D}_{r,y} \\ & + \rho I_z \mathbf{H}_{r,z}^T \mathbf{D}_{r,z} \end{aligned} \quad (18)$$

in which

$$\begin{aligned} \mathbf{H}_{r,y} = & \mathbf{H}_r(cy \mathbf{g}_y), \mathbf{H}_{r,z} = \mathbf{H}_r(cz \mathbf{g}_z) \\ \mathbf{D}_{r,y} = & \mathbf{D}_r(cy \mathbf{g}_y), \mathbf{D}_{r,z} = \mathbf{D}_r(cz \mathbf{g}_z) \end{aligned}$$

where

$$\mathbf{g}_y = [0 \ 1 \ 0]^T \quad \mathbf{g}_z = [0 \ 0 \ 1]^T$$

The virtual external power of the beam element caused by gravity  $\mathbf{I}\mathbf{g}$  can be expressed as

$$\begin{aligned} p_{\text{ext},g} = & \iiint_V \delta \dot{\mathbf{r}}^T \rho \mathbf{I}\mathbf{g} dV \\ = & \rho A \int_0^L \delta \begin{bmatrix} d\mathbf{q}_B \\ d\mathbf{q}_{\text{d},c} \end{bmatrix}^T \mathbf{H}_t^T ds \mathbf{I}\mathbf{g} \end{aligned} \quad (19)$$

### 2.1.6 Discretization

To avoid shear lock, one complex shape function is proposed (Bazoune et al. 2003).

$$\mathbf{q}_{\text{d},c} = \mathbf{N}_c \mathbf{q}_{\text{d},\text{end}} \quad (20)$$

With this shape function, the integration part of internal power become zero (Luo 2008). So that the internal power can be written as

$$\begin{aligned} \delta p_{\text{int}} \\ = & -\delta \dot{\mathbf{q}}_{\text{d},\text{end}}^T \mathbf{N}_c^T (\mathbf{H}_1 \mathbf{N}'_c + \mathbf{H}_2 \mathbf{N}_c) \Big|_0^L \mathbf{q}_{\text{d},\text{end}} \end{aligned} \quad (21)$$

Additionally, using the relationship between deformation coordinate of end point, co-rotational coordinate and generalized coordinate of the beam, we can get

$$\begin{aligned} \begin{bmatrix} d\mathbf{q}_B \\ d\mathbf{q}_{\text{d},c} \end{bmatrix} &= \mathbf{N}_{\text{B},\text{end}} \mathbf{T}_{\text{B},\text{end}} d\mathbf{q}_e \\ \begin{bmatrix} d\dot{\mathbf{q}}_B \\ d\dot{\mathbf{q}}_{\text{d},c} \end{bmatrix} &= \mathbf{N}_{\text{B},\text{end}} \mathbf{T}_{\text{B},\text{end}} d\dot{\mathbf{q}}_e \\ &+ \mathbf{N}_{\text{B},\text{end}} \dot{\mathbf{T}}_{\text{B},\text{end}} d\mathbf{q}_e \end{aligned} \quad (22)$$

in which

$$\begin{aligned} \mathbf{N}_{\text{B},\text{end}} &= \begin{bmatrix} \mathbf{I} & \mathbf{0} \\ \mathbf{0} & \mathbf{N}_c \end{bmatrix} \\ \mathbf{T}_{\text{B},\text{end}} &= \begin{bmatrix} \mathbf{T}_B \\ \mathbf{T}_{\text{d},\text{end}} \end{bmatrix} \quad \dot{\mathbf{T}}_{\text{B},\text{end}} = \begin{bmatrix} \dot{\mathbf{T}}_B \\ \dot{\mathbf{T}}_{\text{d},\text{end}} \end{bmatrix} \end{aligned}$$

The virtual total power of Spatial Timoshenko Beam can be written as

$$\delta p_e = -\delta d\mathbf{q}_e^T (\mathbf{M}_e d\dot{\mathbf{q}}_e + \mathbf{F}_e) \quad (23)$$

The mass matrix regarding to generalized coordinate of beam element can be written as

$$\mathbf{M}_e = \mathbf{T}_{\text{B},\text{end}}^T \int_0^L \mathbf{N}_{\text{B},\text{end}}^T \mathbf{M}_{\text{B},c} \mathbf{N}_{\text{B},\text{end}} ds \mathbf{T}_{\text{B},\text{end}} \quad (24)$$

The force vector regarding to generalized coordinate of beam element can be written as

$$\mathbf{F}_e = \mathbf{D}_e d\mathbf{q}_e + \mathbf{F}_{\text{int},e} + \mathbf{F}_{\text{ext},e,g} \quad (25)$$

in which

$$\begin{aligned} \mathbf{D}_e &= \mathbf{T}_{\text{B},\text{end}}^T \int_0^L \mathbf{N}_{\text{B},\text{end}}^T (\mathbf{M}_{\text{B},c} \mathbf{N}_{\text{B},\text{end}} \dot{\mathbf{T}}_{\text{B},\text{end}} \\ &+ \mathbf{D}_{\text{B},c} \mathbf{N}_{\text{B},\text{end}} \mathbf{T}_{\text{B},\text{end}}) ds \\ \mathbf{F}_{\text{int},e} &= \mathbf{T}_{\text{d},\text{end}}^T \mathbf{N}_c^T (\mathbf{H}_1 \mathbf{N}'_c + \mathbf{H}_2 \mathbf{N}_c) \Big|_0^L \mathbf{q}_{\text{d},\text{end}} \\ \mathbf{F}_{\text{ext},e,g} &= -\mathbf{T}_{\text{B},\text{end}}^T \int_0^L \mathbf{N}_{\text{B},\text{end}}^T \mathbf{H}_t^T \rho A ds \mathbf{I}\mathbf{g} \end{aligned}$$

## 2.2 Super Truss Element

### 2.2.1 Assumptions

In order to reduce the number of degrees of freedom of the truss element, we propose three assumptions so that each beam in the truss element can be expressed by the coordinates of the two end sections. These assumptions can be acceptable when the truss is long and the deformation is uniform and small.

**Assumption 1: Rigid End Section.** When the truss is long, the deformation is mainly along the length of the truss, while the deformation of the end section is relatively small. In reality, the truss is often strengthened on the end section, making the stiffness of the end section larger, so we can consider the end section of the truss to be rigid (Wang et al. 2015). The rigid end section of the truss means the position vector from the section node to any point on the end section in this section coordinate is constant

**Assumption 2: Geometric Continuity of Main Beam.** We assume that after the main beam is deformed, the position vector of its cross-section centre is continuous. Moreover, the arc-length derivative of position vector remains parallel to the normal direction of the cross-section.

**Assumption 3: Rigid Connection.** The rigid connection hypothesis refers to the relative rotation angles of different beam elements connected to the same node in the local coordinate of this end point of the beam, which remain unchanged before and after deformation. In reality, riveting or welding is often used to connect the beam element, and the stiffness of the nodes will be strengthened, so this assumption is in line with the actual situation.

### 2.2.2 Parameterization

**Truss Elements and Truss Order.** In this paper, the truss is defined by nodes (cross section nodes, internal nodes), planes (cross section, sub-beam planes) and beam elements (cross section beams, main beams, sub-beams).

The configuration of the sub-beams is defined by the connection form and the truss order. The sub-beam connection form refers to the position of the internal nodes connected by the sub-beam. Truss order refers to the ratio of the total length of the main beam to the minimum element length divided by the sub-beams.

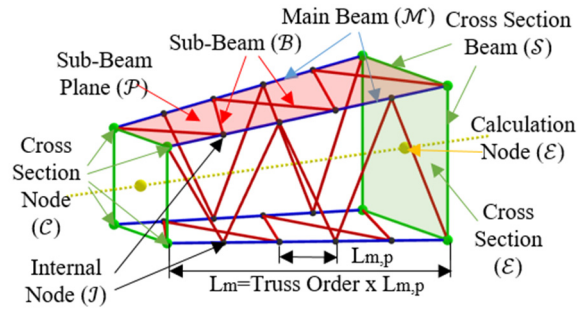


Figure 1: Definition of truss elements and truss order.

**Parameters of Cross Section Nodes.** According to the rigid end section assumption, we only need to define the position vector from the section node to any point on the end section in this section coordinate.

Moreover, the posture of the section node can be expressed by the angle of the end section.

**Parameters of Cross Section Beams.** The cross section beams of a certain cross section  $s$  can be defined by the cross-section nodes.

According to the definition of beam element above, it is required that the x-axis of the beam must be parallel to the line connecting the two ends of the beam when there is no deformation.

The generalized coordinates of the section node can be expressed by the generalized coordinates of the end section

$$\begin{aligned} {}_1\mathbf{n}_x^s &= \Delta_1\mathbf{r}^s / \|\Delta_1\mathbf{r}^s\| \\ \Delta_1\mathbf{r}^s &= {}_1\mathbf{r}^k - {}_1\mathbf{r}^l \end{aligned} \quad (26)$$

in which  $s \in \mathcal{S}$ ,  $k, l \in \mathcal{C}$ .

In addition, we define that the z-axis of cross section beam is perpendicular to the cross section, that is, the same as the x-axis of the cross-section coordinate.

$${}_1\mathbf{n}_z^s = {}_1\mathbf{n}_x^i \quad (27)$$

in which  $i \in \mathcal{E}$ .

Therefore, the rotation matrix of the nodes at both ends of the end beam can be defined as

$$\mathbf{R}_s = [{}_1\mathbf{n}_x^s \quad {}_1\mathbf{n}_y^s \quad {}_1\mathbf{n}_z^s] \quad (28)$$

According to assumption of rigid end section or rigid connection, the relative rotation angle between the coordinate system of the nodes at both ends of the cross-section beam and the coordinate system of the end section is constant under deformation.

$$\mathbf{R}_1^T \mathbf{R}_s \rightarrow {}_1\boldsymbol{\varphi}^{l,s} = \text{constant} \quad (29)$$

**Parameters of Main Beams, Sub-beam Planes and Internal Nodes.** Main beam is defined by the two cross section nodes of different end section.

The x-axis of the main beam is along the length of the main beam

$$\begin{aligned} {}_1\mathbf{n}_x^m &= \Delta_1\mathbf{r}^m / \|\Delta_1\mathbf{r}^m\| \\ \Delta_1\mathbf{r}^m &= {}_1\mathbf{r}^k - {}_1\mathbf{r}^l \end{aligned} \quad (30)$$

in which  $m \in \mathcal{M}$

The sub-beams must be located on the surface formed by the two main beams. We only discuss the situation where two main beams form a plane, which is basically the same in practical applications. The direction of the sub-beam plane and the z-axis of the main beam in this sub-beam plane is defined by its normal vector.

$$\begin{aligned} {}_1\mathbf{k}^g &= {}_1\mathbf{n}_x^m \times {}_1\mathbf{n}_z^n \\ {}_1\mathbf{n}_z^{m,g} &= {}_1\mathbf{n}_z^n = {}_1\mathbf{k}^g \end{aligned} \quad (31)$$

in which  $n \in \mathcal{M}$ ,  $g \in \mathcal{P}$ .

The main beams belonging to different sub-beam planes will have different directions defined in each sub-beam plane. According to the rigid connection assumption, the relative rotation angle between the end node of the main beam and the cross-section node is constant.

$${}_i\boldsymbol{\varphi}^{m,g} = {}_i\boldsymbol{\varphi}^{m,g}(\mathbf{R}_i^T \mathbf{R}_{m,g}) \quad (32)$$

With the assumption of geometric continuity of the main beam, the direction of the internal nodes on the main beam is the same as the direction of the main beam when it is not deformed.

**Parameters of Sub-beams.** The sub-beam is defined by the main beam and the location of end nodes on the main beam.

The x-axis of the sub-beam is defined as the unit vector from the internal node on main beam 1 point to the internal node on main beam 2.

$$\begin{aligned} {}_1\mathbf{n}_x^h &= \Delta_1\mathbf{r}^h / \|\Delta_1\mathbf{r}^h\| \\ \Delta_1\mathbf{r}^h &= {}_1\mathbf{r}^{m,p} - {}_1\mathbf{r}^{n,q} \end{aligned} \quad (33)$$

in which  $h \in \mathcal{B}$ ,  $p, q \in \mathcal{I}$ .

The z-axis of the sub-beam is defined as the normal direction of the sub-beam plane.

$${}_1\mathbf{n}_z^h = {}_1\mathbf{k}^g \quad (34)$$

According to the rigid connection assumption, the relative rotation angle between the end point coordinate of the sub-beam and the corresponding main beam coordinate is constant and must be along the normal direction of the sub-beam plane.

$$\mathbf{R}_m^T \mathbf{R}_h \rightarrow {}_m\boldsymbol{\varphi}^{h,m} = {}_m\boldsymbol{\varphi}^{h,m} {}_1\mathbf{k}^g \quad (35)$$

### 2.2.3 Calculation

The dynamics calculation of the super truss element is composed of the following modules: cross section node, internal node, cross section beam, main beam and sub-beam.

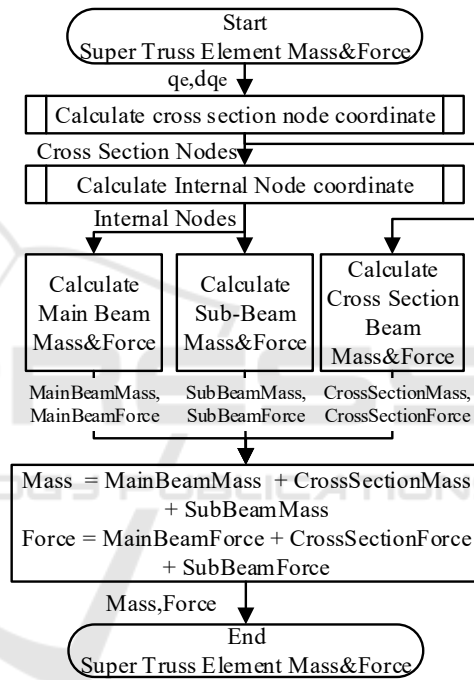


Figure 2: Flow chart of dynamic calculation of super truss element.

From the dynamic calculation flow chart, it can be found that the calculations of the cross-section beam, the main beam and the sub-beams do not affect each other. Parallel calculation can effectively reduce the single-step calculation time of the super truss element.

**Cross Section Nodes.** According to the assumption of rigid end section, the position of the cross-section nodes can be calculated. Moreover, the posture of the section nodes can be expressed by the angle of the end section. Therefore, the generalized coordinates of the section node can be expressed by the generalized coordinates of the end section

$$\mathbf{q}_k = \begin{bmatrix} \mathbf{r}^k \\ \boldsymbol{\varphi}^k \end{bmatrix} = \begin{bmatrix} \mathbf{r}^i + \mathbf{R}_{ii}\mathbf{r}^{i,k} \\ \boldsymbol{\varphi}^i \end{bmatrix} \quad (36)$$

$$\mathbf{R}_i = \mathbf{R}(\boldsymbol{\varphi}^i)$$

The generalized velocity and acceleration of the cross-section node can be expressed as

$$\begin{aligned} d\mathbf{q}_k &= \begin{bmatrix} \mathbf{r}^k \\ \boldsymbol{\varphi}^k \end{bmatrix}^T = \mathbf{T}_k d\mathbf{q}_e \\ d\dot{\mathbf{q}}_k &= \mathbf{T}_k d\dot{\mathbf{q}}_e + \dot{\mathbf{T}}_k d\mathbf{q}_e \end{aligned} \quad (37)$$

in which

$$\mathbf{T}_k = \mathbf{T}_k^i \mathbf{T}_i \quad \dot{\mathbf{T}}_k = \dot{\mathbf{T}}_k^i \mathbf{T}_i$$

where

$$\begin{aligned} \mathbf{T}_k^i &= \begin{bmatrix} \mathbf{I} & -\mathbf{R}_{ii}\tilde{\mathbf{r}}^{i,k} \\ \mathbf{0} & \mathbf{I} \end{bmatrix} \\ \dot{\mathbf{T}}_k^i &= \begin{bmatrix} \mathbf{0} & -\mathbf{R}_{ii}\tilde{\boldsymbol{\omega}}^i\tilde{\mathbf{r}}^{i,k} \\ \mathbf{0} & \mathbf{0} \end{bmatrix} \end{aligned}$$

and  $\mathbf{T}_i$  is the selection matrix of the end section.

$$\mathbf{T}_i = \begin{cases} [\mathbf{I} & \mathbf{0}], & i = 1 \\ [\mathbf{0} & \mathbf{I}], & i = 2 \end{cases}$$

**Internal Nodes.** Here the main deformation of the main beam is considered to be caused by bending. Thus, the deformation in axial direction is ignored (Zhang et al. 2015). The global position vector of centreline is obtained by employing the Hermite interpolation. The velocity and acceleration of the centroid can be expressed as

$$\begin{aligned} \dot{\mathbf{r}}^p &= \mathbf{T}_r d\mathbf{q}_m \\ \ddot{\mathbf{r}}^p &= \mathbf{T}_r d\dot{\mathbf{q}}_m + \dot{\mathbf{T}}_r d\mathbf{q}_m \end{aligned} \quad (38)$$

In order to determine the angle coordinates, we use the cardan angle to describe the angle change relative to the end of Section 1

$$\begin{array}{ccc} z & y & x \\ k \rightarrow & \rightarrow & \rightarrow p \\ \theta & \psi & \varphi \end{array} \quad \begin{array}{ccc} z & y & x \\ k \rightarrow & \rightarrow & \rightarrow l \\ \theta^{12} & \psi^{12} & \varphi^{12} \end{array}$$

So that the rotation matrix of cross section can be formulated as

$$\mathbf{R}_p = \mathbf{R}_k \mathbf{R}_z(\theta) \mathbf{R}_y(\psi) \mathbf{R}_x(\varphi) \quad (39)$$

According to Hermite Interpolation, the unit normal vector of the cross-section can be expressed by

$$\mathbf{n}_x^p = \mathbf{r}'^p / \|\mathbf{r}'^p\| \quad (40)$$

The unit normal vector of the cross-section can also be expressed through the relative rotation angle to end section 1

$$\mathbf{n}_x^p = \mathbf{R}_k \mathbf{R}_z(\theta) \mathbf{R}_y(\psi) \mathbf{g}_x \quad (41)$$

Since the relative rotation angle is small, according to the monotonicity of the sin-function near zero position, two parameters of the cardan angle can be obtained by the following formula

$$\begin{aligned} \psi &= -\sin^{-1}(\mathbf{g}_z^T \mathbf{R}_k^T \mathbf{n}_x^p) \\ \theta &= \sin^{-1}\left(\frac{\mathbf{g}_y^T \mathbf{R}_k^T \mathbf{n}_x^p}{\cos \psi}\right) \end{aligned} \quad (42)$$

The torsion angle in the x direction is obtained by linear interpolation

$$\varphi = \xi_1 \varphi^{12} \quad \dot{\varphi} = \xi_1 \dot{\varphi}^{12} \quad (43)$$

The torsion angle from end section 1 to end section 2 can be obtained by solving following equation

$$\mathbf{R}_l = \mathbf{R}_k \mathbf{R}_z(\theta^{12}) \mathbf{R}_y(\psi^{12}) \mathbf{R}_x(\varphi^{12}) \quad (44)$$

The solution is

$$\begin{aligned} \varphi^{12} &= \sin^{-1}\left(\frac{\mathbf{g}_z^T \mathbf{R}_k^T \mathbf{R}_l \mathbf{g}_x}{\cos \psi^{12}}\right) \\ \psi^{12} &= -\sin^{-1}(\mathbf{g}_z^T \mathbf{R}_k^T \mathbf{R}_l \mathbf{g}_x) \\ \theta^{12} &= \sin^{-1}\left(\frac{\mathbf{g}_y^T \mathbf{R}_k^T \mathbf{R}_l \mathbf{g}_x}{\cos \psi^{12}}\right) \end{aligned} \quad (45)$$

in which  $\mathbf{g}_x = [1 \ 0 \ 0]^T$ .

Angular deformation vector related to cardan angle can be written as

$$\boldsymbol{\varphi} = [\varphi \ \psi \ \theta]^T \quad (46)$$

According to the relationship between rotation matrix and the Cartesian rotation vector, the rotation vector  $\boldsymbol{\varphi}^p$  of cross section can be obtained by

$$\mathbf{R}_p \rightarrow \boldsymbol{\varphi}^p \quad (47)$$

The angular velocity and angular acceleration of section  $c$  can be written as

$$\begin{aligned} {}_p\boldsymbol{\omega}^p &= \mathbf{T}_\omega d\mathbf{q}_m = \mathbf{R}_{\varphi k}^T \boldsymbol{\omega}^k + \mathbf{T}_{\varphi 1} \dot{\boldsymbol{\varphi}} \\ {}_p\dot{\boldsymbol{\omega}}^p &= \mathbf{R}_{\varphi k}^T \dot{\boldsymbol{\omega}}^k - {}_p\tilde{\boldsymbol{\omega}}^p \mathbf{R}_{\varphi k}^T \boldsymbol{\omega}^k + \dot{\mathbf{T}}_{\varphi 1} \dot{\boldsymbol{\varphi}} \\ &\quad + \mathbf{T}_{\varphi 1} \ddot{\boldsymbol{\varphi}} = \mathbf{T}_\omega d\dot{\mathbf{q}}_m + \dot{\mathbf{T}}_\omega d\mathbf{q}_m \end{aligned} \quad (48)$$

in which the rotation matrix and angular velocity with subscript  $\varphi$  should be calculated using cardan angle

The generalized coordinate and generalized velocity of internal node of main beam can be obtained by

$$\begin{aligned} \mathbf{q}_p &= [{}_1\mathbf{r}^{pT} \quad \boldsymbol{\varphi}^{pT}]^T \\ d\mathbf{q}_p &= [{}_1\dot{\mathbf{r}}^{pT} \quad {}_p\boldsymbol{\omega}^{pT}]^T = \mathbf{T}_p^m d\mathbf{q}_m \\ d\dot{\mathbf{q}}_p &= \mathbf{T}_p^m d\dot{\mathbf{q}}_m + \dot{\mathbf{T}}_p^m d\mathbf{q}_m \end{aligned} \quad (49)$$

where

$$\mathbf{T}_p^m = [\mathbf{T}_r^T \quad \mathbf{T}_\omega^T]^T \quad \dot{\mathbf{T}}_p^m = [\dot{\mathbf{T}}_r^T \quad \dot{\mathbf{T}}_\omega^T]^T$$

According to the definition of the main beam, the coordinate of end point of the main beam can be represented by the end node coordinate of super truss element.

$$\begin{aligned} d\mathbf{q}_m &= \mathbf{T}_m d\mathbf{q}_e \\ d\dot{\mathbf{q}}_m &= \mathbf{T}_m d\dot{\mathbf{q}}_e + \dot{\mathbf{T}}_m d\mathbf{q}_e \end{aligned} \quad (50)$$

where

$$\mathbf{T}_m = [\mathbf{T}_k^T \quad \mathbf{T}_l^T]^T \quad \dot{\mathbf{T}}_m = [\dot{\mathbf{T}}_k^T \quad \dot{\mathbf{T}}_l^T]^T$$

Therefore, the internal node coordinate can be written by the coordinate of the super truss beam element.

$$\begin{aligned} d\mathbf{q}_p &= \mathbf{T}_p d\mathbf{q}_e \\ d\dot{\mathbf{q}}_p &= \mathbf{T}_p d\dot{\mathbf{q}}_e + \dot{\mathbf{T}}_p d\mathbf{q}_e \end{aligned} \quad (51)$$

where

$$\mathbf{T}_p = \mathbf{T}_p^m \mathbf{T}_m \quad \dot{\mathbf{T}}_p = \mathbf{T}_p^m \dot{\mathbf{T}}_m + \dot{\mathbf{T}}_p^m \mathbf{T}_m$$

**Cross Section Beam Elements.** According to the parameters of the definition of cross section nodes, the coordinate of the end point of the cross-section beam is depend only on cross section node.

$$\mathbf{q}_s^k = \begin{bmatrix} {}_1\mathbf{r}_s^k \\ \boldsymbol{\varphi}_s^k \end{bmatrix} = \begin{bmatrix} {}_1\mathbf{r}^k \\ \boldsymbol{\varphi}^i + \mathbf{R}_{i_1} \boldsymbol{\varphi}^{s,i} \end{bmatrix} \quad (52)$$

The generalized velocity and acceleration of the end point of the cross-section beam can be expressed as

$$\begin{aligned} d\mathbf{q}_s^k &= \begin{bmatrix} {}_1\dot{\mathbf{r}}^{s,k} \\ {}_k\boldsymbol{\omega}_s^k \end{bmatrix} = \mathbf{T}_{s,k} d\mathbf{q}_e \\ d\dot{\mathbf{q}}_s^k &= \mathbf{T}_{s,k} d\dot{\mathbf{q}}_e + \dot{\mathbf{T}}_{s,k} d\mathbf{q}_e \end{aligned} \quad (53)$$

where

$$\begin{aligned} \mathbf{T}_{s,k} &= \mathbf{T}_{s,k}^k \mathbf{T}_k \quad \dot{\mathbf{T}}_{s,k} = \mathbf{T}_{s,k}^k \dot{\mathbf{T}}_k \\ \mathbf{T}_{s,k}^k &= \begin{bmatrix} \mathbf{I} & \mathbf{0} \\ \mathbf{0} & \mathbf{R}^T({}_i\boldsymbol{\varphi}^{s,i}) \end{bmatrix} \end{aligned}$$

According to the definition of end beam, the generalized coordinates of end beam can be expressed as

$$\begin{aligned} \mathbf{q}_s &= [\mathbf{q}_s^{kT} \quad \mathbf{q}_s^{lT}]^T \\ d\mathbf{q}_s &= [d\mathbf{q}_s^{kT} \quad d\mathbf{q}_s^{lT}]^T = \mathbf{T}_s d\mathbf{q}_e \\ d\dot{\mathbf{q}}_s &= \mathbf{T}_s d\dot{\mathbf{q}}_e + \dot{\mathbf{T}}_s d\mathbf{q}_e \end{aligned} \quad (54)$$

where

$$\begin{aligned} \mathbf{T}_s &= [\mathbf{T}_{s,k}^T \quad \mathbf{T}_{s,l}^T]^T \\ \dot{\mathbf{T}}_s &= [\dot{\mathbf{T}}_{s,k}^T \quad \dot{\mathbf{T}}_{s,l}^T]^T \end{aligned}$$

The mass matrix and force vector of the cross-section beam need to be calculated through the generalized coordinates of the cross-section beam, and then converted to the super truss element coordinate. The virtual power of the cross-section beam can be written as

$$\begin{aligned} \delta p_e^s &= -\delta d\mathbf{q}_s^T (\mathbf{M}_s^s d\dot{\mathbf{q}}_s + \mathbf{F}_s^s) \\ &= -\delta d\mathbf{q}_e^T (\mathbf{M}_e^s d\dot{\mathbf{q}}_e + \mathbf{F}_e^s) \end{aligned} \quad (55)$$

where

$$\begin{aligned} \mathbf{M}_e^s &= \mathbf{T}_s^T \mathbf{M}_s^s \mathbf{T}_s \\ \mathbf{F}_e^s &= \mathbf{T}_s^T (\mathbf{M}_s^s \mathbf{T}_s d\mathbf{q}_e + \mathbf{F}_s^s) \end{aligned}$$

**Main Beam Elements.** Considering that internal nodes will transmit force and moment, it is necessary to segment the main beam according to the position of the internal nodes (sub main beam), in order to meet the virtual power principle. The generalized coordinate of sub main beam can be obtained directly using the generalized coordinate of internal nodes.



$$\begin{aligned} d\mathbf{q}_m &= \mathbf{T}_m d\mathbf{q}_e \\ d\dot{\mathbf{q}}_m &= \mathbf{T}_m d\dot{\mathbf{q}}_e + \dot{\mathbf{T}}_m d\mathbf{q}_e \end{aligned} \quad (56)$$

where

$$\mathbf{T}_m = [\mathbf{T}_p^T \quad \mathbf{T}_q^T]^T \quad \dot{\mathbf{T}}_m = [\dot{\mathbf{T}}_p^T \quad \dot{\mathbf{T}}_q^T]^T \quad (57)$$

The virtual power of sub main beam can be written as

$$\begin{aligned} \delta p_e^m &= -\delta d\mathbf{q}_m^T (\mathbf{M}_m^m d\dot{\mathbf{q}}_m + \mathbf{F}_m^m) \\ &= -\delta d\mathbf{q}_e^T (\mathbf{M}_e^m d\dot{\mathbf{q}}_e + \mathbf{F}_e^m) \end{aligned} \quad (58)$$

where

$$\begin{aligned} \mathbf{M}_e^m &= \mathbf{T}_m^T \mathbf{M}_m^m \mathbf{T}_m \\ \mathbf{F}_e^m &= \mathbf{T}_m^T (\mathbf{M}_m^m \dot{\mathbf{T}}_m d\mathbf{q}_e + \mathbf{F}_m^m) \end{aligned}$$

**Sub-beam Elements.** According to the internal nodes connected by the sub-beam and the constant relative rotation between the end points of the sub-beam and the internal nodes, the generalized coordinates of the end points of the sub-beam can be obtained through the internal nodes.

The generalized velocity and acceleration of the sub-beam endpoint can be expressed as

$$\begin{aligned} d\mathbf{q}_h^p &= \mathbf{T}_{h,p} d\mathbf{q}_e \\ d\dot{\mathbf{q}}_h^p &= \mathbf{T}_{h,p} d\dot{\mathbf{q}}_e + \dot{\mathbf{T}}_{h,p} d\mathbf{q}_e \end{aligned} \quad (59)$$

where

$$\begin{aligned} \mathbf{T}_{h,p} &= \mathbf{T}_{h,p}^p \mathbf{T}_p \quad \dot{\mathbf{T}}_{h,p} = \mathbf{T}_{h,p}^p \dot{\mathbf{T}}_p \\ \mathbf{T}_{h,p}^p &= \begin{bmatrix} \mathbf{I} & \mathbf{0} \\ \mathbf{0} & \mathbf{R}^T(\mathbf{p}\boldsymbol{\varphi}^{h,p}) \end{bmatrix} \end{aligned}$$

Therefore, the generalized coordinates of sub-beam can be written as

$$\begin{aligned} d\mathbf{q}_h &= \mathbf{T}_h d\mathbf{q}_e \\ d\dot{\mathbf{q}}_h &= \mathbf{T}_h d\dot{\mathbf{q}}_e + \dot{\mathbf{T}}_h d\mathbf{q}_e \end{aligned} \quad (60)$$

where

$$\mathbf{T}_h = [\mathbf{T}_{h,p}^T \quad \mathbf{T}_{h,q}^T]^T \quad \dot{\mathbf{T}}_h = [\dot{\mathbf{T}}_{h,p}^T \quad \dot{\mathbf{T}}_{h,q}^T]^T$$

The virtual power of sub-beam can be written as

$$\begin{aligned} \delta p_e^h &= -\delta d\mathbf{q}_h^T (\mathbf{M}_h^h d\dot{\mathbf{q}}_h + \mathbf{F}_h^h) \\ &= -\delta d\mathbf{q}_e^T (\mathbf{M}_e^h d\dot{\mathbf{q}}_e + \mathbf{F}_e^h) \end{aligned} \quad (61)$$

where

$$\begin{aligned} \mathbf{M}_e^h &= \mathbf{T}_h^T \mathbf{M}_h^h \mathbf{T}_h \\ \mathbf{F}_e^h &= \mathbf{T}_h^T (\mathbf{M}_h^h \dot{\mathbf{T}}_h d\mathbf{q}_e + \mathbf{F}_h^h) \end{aligned}$$

### 3 SIMULATION AND ANALYSIS

#### 3.1 Model of a Lattice Boom System

This lattice boom system of a mobile crane consists of a main boom, a derrick boom, strut tie rods and ropes. The model is created using rigid-flexible multibody dynamics method.

The configurations of body model type and joint are shown in Figure 3.

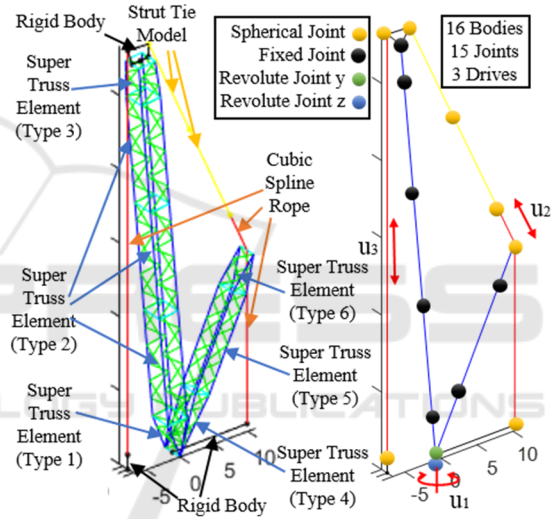


Figure 3: Element Type (left, real model) and Joint Configuration (right, calculation model).

The lattice boom system has now three drives: 1. crane rotates along z-axis. 2. lift rope changes its length. 3. angle of main boom changes.

The types of the truss elements are shown in Figure 4.

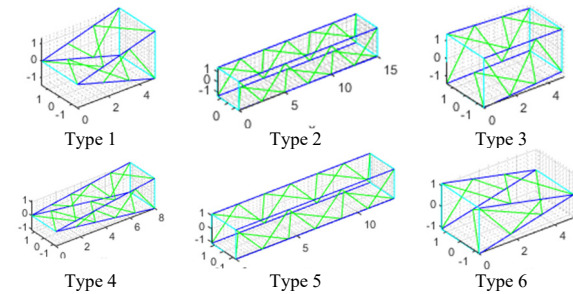


Figure 4: Different Types of Super Truss Element.

### 3.2 Dynamics Tests for Truss Element

If we fix one end of the super truss element and apply force or torque on the other end, the displacement of the free end can reflect the stiffness of the truss beam. Here in Figure 5 only the curves of external force or torque and strain of Type 2 are shown as an example.

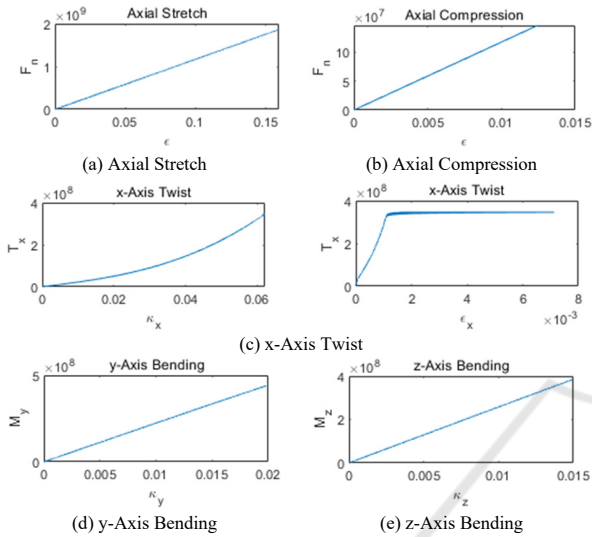


Figure 5: Strain-stress curves under different deformation states for super truss element Type 2.

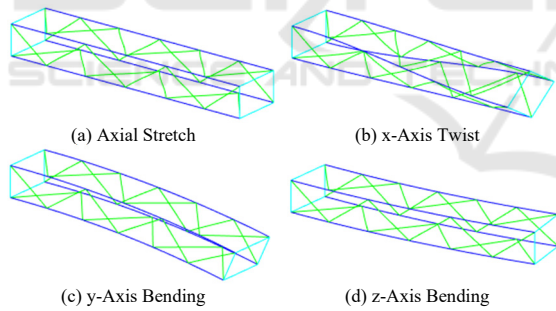


Figure 6: Deformation in different states for super truss element Type 2.

It can be seen from the curve in Figure 5 that the stresses and strains by axial force and bending are linear. The torsion in the x-axis will cause the strain in the axial direction, which is caused by the main beam rotating around the axis of super truss element instead of its own axis. This also makes the equivalent torsional stiffness in x-axis of the truss not constant. The continuous beam model cannot express this phenomenon. The state after the deformation of the super truss element under various conditions is shown in Figure 6.

If we let the both end of the super truss element free and add same force or torque on both ends. The

velocity change of the super truss element can be used to determine the mass parameter.

From Figure 7, the angular velocity change can be seen as linear to time. However, only the translational velocity change in x-Axis is linear to time. In fact, due to the discontinuity and asymmetry of the truss, it is difficult to express the mass matrix of the truss through a continuous beam model. Especially for non-rectangular trusses, the determination of its equivalent mass will become very difficult.

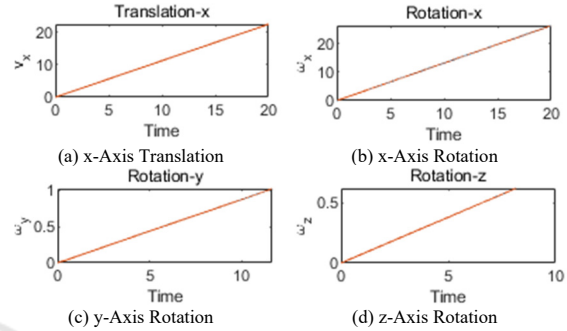


Figure 7: Time-Velocity curves under different force or torque states for super truss element Type 2.

### 3.3 Load Lifting

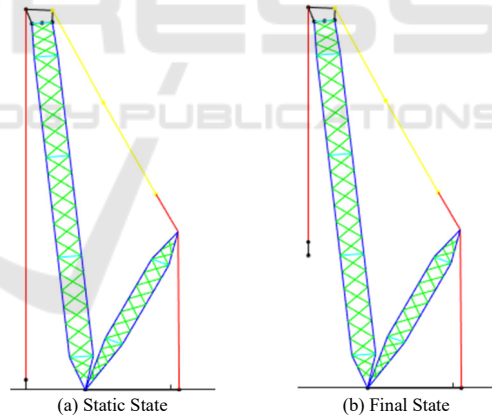


Figure 8: Start State (a) and Final State (b) for lifting.

The actual motion of the crane must be relatively smooth. In order to simulate smooth motion, we will use the motion function in (Gao et al. 2020) to lift the load. The start state and final state for lifting is shown in Figure 8.

The translational displacement and velocity in z-axis are shown in Figure 9.

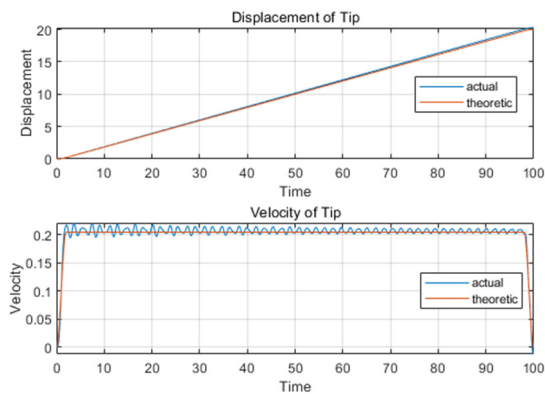


Figure 9: translational displacement and velocity in z-axis for lifting.

### 3.4 Combined Motion

In practice, the motions of the mobile cranes in the operation can be specified as three kinds, lifting, slewing, and luffing. The slewing means the boom system and the turntable (super-structure) rotates along the vertical slewing axis. The luffing means to change the distance between the payload and the slewing axis by changing the elevation angle of the boom. In this section, we also designed the lifting state under the simultaneous action of multiple drives. The combined motion can be divided into 4 stages:

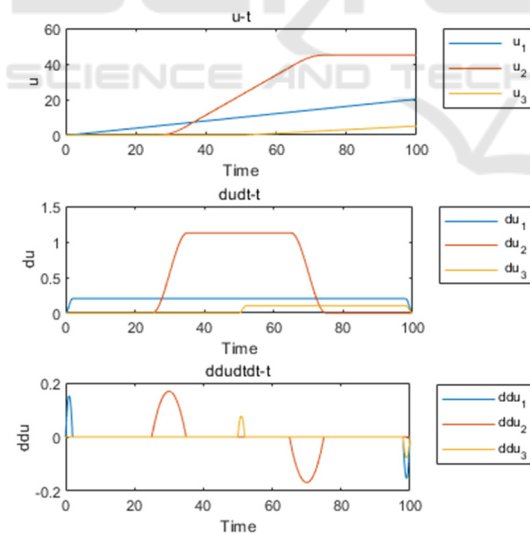


Figure 10: Combined Drive Function.

1. 0 - 25s: lifting stage
2. 25 - 50s: lifting + slewing stage
3. 50 - 75s: lifting + slewing + luffing stage
4. 75 - 100s: lifting + luffing stage

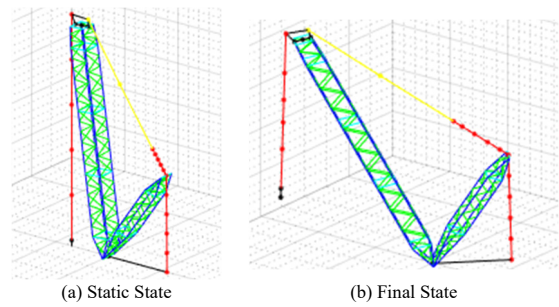


Figure 11: Start State (a) and Final State (b) for combined motion.

During the movement, the position and speed of the load are shown in Figure 12. From the figure, we can find that in the only lifting stage, the position of the load changes smoothly, and the speed has only a small vibration. The slewing of the crane has little effect on the vertical motion of the load. The position of the load changes smoothly in the horizontal direction, but speed begins to fluctuate greatly. The luffing motion of the crane has a greater influence on the vertical direction of the lifting, the fluctuation of the speed in the vertical direction becomes larger, and there is a big vibration in the horizontal direction.

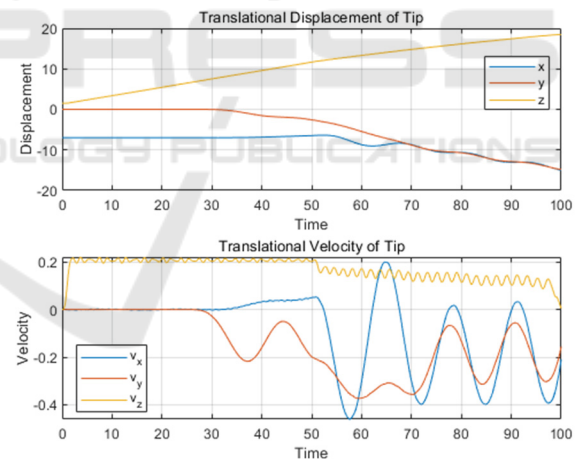


Figure 12: Translational Position and Velocity of the Load.

For some kinds of loads, the stability of its posture is also very important. Therefore, in addition to the position change of the load, we also need to consider the angle change when it is moving. The angle change is shown in Figure 13. We can find that in the overall movement, the angle of the load does not change much (the maximum angle change is less than 1 degree). Among them, the angle change caused by the forward motion of the crane is relatively the largest, and the angular velocity of the load vibrates violently.

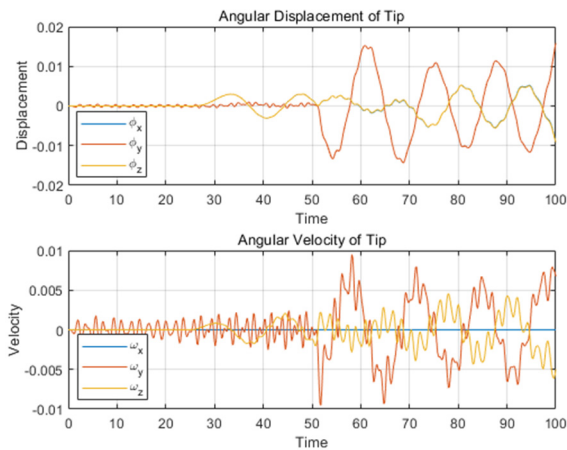


Figure 13: Posture and Angular Velocity of the Load.

## 4 CONCLUSION AND OUTLOOK

In order to reduce the complexity of truss beam modelling in this paper a super truss element for dynamic calculation is proposed. Based on three assumptions, a parameterization method for truss beams is established, and a dynamic calculation method for super truss elements is proposed.

Through the stiffness experiment of super truss elements, a reasonable method to determine the properties of truss beams is given, and the problem of using continuous beam elements to simulate truss beam elements has been discovered. Finally, through the crane movement, the feasibility of using super truss element modelling was confirmed.

The following topics are considered as further research:

1) Although the super truss element can greatly reduce the number of degrees of freedom, it is still needed to calculate each member of the truss beam in each time step. This makes the single-step calculation time of the ODE solver very large. Parallel computing and other methods of accelerating computing to reduce computing time will be studied in the future.

2) The parameterization method in this paper is only suitable for general simple truss models. At present, in the direction of lighter and miniaturized machinery, more complex truss models are widely used. These trusses may no longer meet the three assumptions in this paper when they are deformed. Therefore, a completer and more general truss model is urgently needed.

## ACKNOWLEDGEMENTS

The research is supported by Deutsche Forschungsgemeinschaft (DFG) (FO 1180 1-1).

## REFERENCES

- Bazoune, A.; Khulief, Y. A.; Stephen, N. G. (2003): Shape functions of three-dimensional Timoshenko beam element. In: *Journal of Sound and Vibration* 259 (2), S. 473–480.
- Gao, Lingchong; Zhuo, Yingpeng; Peng, Micheal Kleeberger; Haijun; Fottner, Johannes (2020): Modeling and Simulation of Long Boom Manipulator Based on Geometrically Exact Beam Theory. In: *Proceedings of the 10th International Conference on Simulation and Modeling Methodologies, Technologies and Applications*, S. 209–216.
- Günthner, W. A.; Kleeberger, M. (1997): Zum Stand der Berechnung von Gittermast-Fahrzeugkranen. In: *dhf* (03), S. 56–61.
- Kammer, Daniel C.; Allen, Mathew S.; Mayes, Randy L. (2015): Formulation of an experimental substructure model using a Craig–Bampton based transmission simulator. In: *Journal of Sound and Vibration* 359, S. 179–194.
- Kleeberger, Michael (1996): Nichtlineare dynamische Berechnung von Gittermast-Fahrzeugkranen: na.
- Kleeberger, Michael; Hübner, Karl-Thomas (2006): Using Superelements in the Calculation of Lattice-Boom Cranes. In: *Logistics Journal: referierte Veröffentlichungen* 2006 (Dezember).
- Koutsovasilis, P.; Beitelschmidt, M. (2007): Model Reduction of Large Elastic Systems: A.
- Luo, Yunhua (2008): An efficient 3d timoshenko beam element with consistent shape functions. In: *Adv. Theor. Appl. Mech* 1 (3), S. 95–106.
- Wang, Gang; Qi, Zhaohui; Kong, Xianchao (2015): Geometrical nonlinear and stability analysis for slender frame structures of crawler cranes. In: *Engineering Structures* 83, S. 209–222.
- Zhang, Zhigang; Qi, Zhaohui; Wu, Zhigang; Fang, Huiqing (2015): A spatial Euler-Bernoulli beam element for rigid-flexible coupling dynamic analysis of flexible structures. In: *Shock and Vibration* 2015.